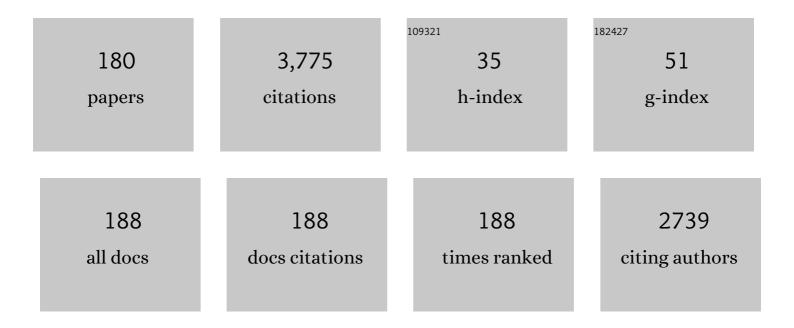
List of Publications by Year in descending order

Source: https://exaly.com/author-pdf/7826312/publications.pdf Version: 2024-02-01



D۸ ш

#	Article	IF	CITATIONS
1	Surface Modification of Bacterial Cellulose for Biomedical Applications. International Journal of Molecular Sciences, 2022, 23, 610.	4.1	43
2	Liquid lithium wetting and percolation in a porous tungsten/liquid Li plasma facing component (PFC). Fusion Engineering and Design, 2022, 178, 113087.	1.9	2
3	HIDRA-MAT liquid metal droplet injector for liquid metal applications in HIDRA. Fusion Engineering and Design, 2022, 180, 113193.	1.9	5
4	<i>Escherichia coli</i> Adhesion and Biofilm Formation on Polydimethylsiloxane are Independent of Substrate Stiffness. Langmuir, 2021, 37, 16-25.	3.5	22
5	High Flux Helium Irradiation of Dispersion-Strengthened Tungsten Alloys and Effects of Heavy Metal Impurity Layer Deposition. Journal of Nuclear Materials, 2021, 544, 152672.	2.7	7
6	Recrystallization suppression through dispersion-strengthening of tungsten. Journal of Nuclear Materials, 2021, 545, 152613.	2.7	8
7	Synergistic Effect of rhBMP-2 Protein and Nanotextured Titanium Alloy Surface to Improve Osteogenic Implant Properties. Metals, 2021, 11, 464.	2.3	7
8	Development of the materials analysis and particle probe for Proto-MPEX. Review of Scientific Instruments, 2021, 92, 045108.	1.3	2
9	Tailoring adaptive bioresorbable Mg-based scaffolds with directed plasma nanosynthesis for enhanced osseointegration and tunable resorption. Applied Surface Science, 2021, 550, 149388.	6.1	7
10	Bacterial Envelope Damage Inflicted by Bioinspired Nanostructures Grown in a Hydrogel. ACS Applied Bio Materials, 2020, 3, 7974-7988.	4.6	22
11	Coherent Atomic-Scale Ripples on Metallic Glasses Patterned by Low-Energy Ion Irradiation for Large-Area Surface Structuring. ACS Applied Nano Materials, 2020, 3, 12025-12033.	5.0	4
12	An Overview of the Hybrid Illinois Device for Research and Applications Material Analysis Test-stand (HIDRA-MAT). Journal of Fusion Energy, 2020, 39, 448-454.	1.2	5
13	Nonlinear compositional and morphological evolution of ion irradiated GaSb prior to nanostructure formation. Scientific Reports, 2020, 10, 8253.	3.3	1
14	In Vitro Bone Cell Behavior on Porous Titanium Samples: Influence of Porosity by Loose Sintering and Space Holder Techniques. Metals, 2020, 10, 696.	2.3	21
15	lon-Induced Nanopatterning of Bacterial Cellulose Hydrogels for Biosensing and Anti-Biofouling Interfaces. ACS Applied Nano Materials, 2020, 3, 6719-6728.	5.0	15
16	GD-OES study of the influence of second phase particles on the deuterium depth distribution in dispersion-strengthened tungsten. Journal of Nuclear Materials, 2020, 532, 152047.	2.7	7
17	Synthesis and Properties of Mg-Based Foams by Infiltration Casting Without Protective Cover Gas. Journal of Materials Engineering and Performance, 2020, 29, 681-690.	2.5	5
18	Low Recycling Divertor for JET Burning Plasma Regime (\$P_{mathrm{DT}} > 25 MW,) Tj ETQq0 0 0 rgBT	Overlock 10/ 1.3	) Tf 50 67 Td ( 4

48, 1849-1856.

#	Article	IF	CITATIONS
19	Bioinspired Interfaces for the Management of Skin Infections. , 2020, , 457-476.		Ο
20	Balancing biofunctional and biomechanical properties using porous titanium reinforced by carbon nanotubes. Journal of Biomedical Materials Research - Part A, 2019, 107, 719-731.	4.0	6
21	Alternative Plasma-Facing-Material Concepts for Extreme Plasma-Burning Nuclear Fusion Environments. Fusion Science and Technology, 2019, 75, 702-718.	1.1	4
22	Elemental Characterization of Neutron-Irradiated Tungsten Using the GD-OES Technique. Fusion Science and Technology, 2019, 75, 510-519.	1.1	0
23	In-operando observation of helium-irradiation ion effects on surface deuterium retention through LiOH bonding in lithium films on tungsten substrates. Nuclear Materials and Energy, 2019, 19, 463-467.	1.3	3
24	Deciphering the role of second phase precipitates on early-stage surface morphology development of dispersion-strengthened W alloys under low energy He irradiation. Nuclear Materials and Energy, 2019, 19, 47-54.	1.3	14
25	NSTX/NSTX-U theory, modeling and analysis results. Nuclear Fusion, 2019, 59, 112007.	3.5	20
26	Pre-Irradiation Comparison of W-Based Alloys for the PHENIX Campaign: Microstructure, Composition, and Mechanical Properties. Fusion Science and Technology, 2019, 75, 533-541.	1.1	0
27	Designing Nanostructured Ti <sub>6</sub> Al <sub>4</sub> V Bioactive Interfaces with Directed Irradiation Synthesis toward Cell Stimulation to Promote Host–Tissue-Implant Integration. ACS Biomaterials Science and Engineering, 2019, 5, 3325-3339.	5.2	13
28	Coatings for biodegradable magnesium-based supports for therapy of vascular disease: A general view. Materials Science and Engineering C, 2019, 102, 150-163.	7.3	63
29	Summary of the FESAC Transformative Enabling Capabilities Panel Report. Fusion Science and Technology, 2019, 75, 167-177.	1.1	7
30	Enzyme-catalysed biodegradation of carbon dots follows sequential oxidation in a time dependent manner. Nanoscale, 2019, 11, 8226-8236.	5.6	38
31	Effect of deuterium irradiation on graphite boronized in the NSTX-U tokamak. Scientific Reports, 2019, 9, 2435.	3.3	6
32	Designing bioactive porous titanium interfaces to balance mechanical properties and in vitro cells behavior towards increased osseointegration. Surface and Coatings Technology, 2019, 368, 162-174.	4.8	48
33	Directed Irradiation Synthesis as an Advanced Plasma Technology for Surface Modification to Activate Porous and "as-received―Titanium Surfaces. Metals, 2019, 9, 1349.	2.3	8
34	In situ Study Unravels Bioâ€Nanomechanical Behavior in a Magnetic Bacterial Nanoâ€cellulose (MBNC) Hydrogel for Neuroâ€Endovascular Reconstruction. Macromolecular Bioscience, 2019, 19, e1800225.	4.1	23
35	Stellarator Research Opportunities: A Report of the National Stellarator Coordinating Committee. Journal of Fusion Energy, 2018, 37, 51-94.	1.2	15
36	Surface treatment of metallic biomaterials in contact with blood to enhance hemocompatibility. , 2018, , 279-326.		7

#	Article	IF	CITATIONS
37	Microstructural and compositional effects of transition metal carbide additions on dispersion-strengthened tungsten fabricated via spark plasma sintering. International Journal of Refractory Metals and Hard Materials, 2018, 75, 279-286.	3.8	31
38	Effect of boronization on plasma-facing graphite surfaces and its correlation with the plasma behavior in NSTX-U. Nuclear Materials and Energy, 2018, 17, 211-216.	1.3	10
39	Deuterium uptake and sputtering of simultaneous lithiated, boronized, and oxidized carbon surfaces irradiated by low-energy deuterium. Journal of Applied Physics, 2018, 123, .	2.5	7
40	Unraveling the surface chemistry processes in lithiated and boronized plasma material interfaces under extreme conditions. Matter and Radiation at Extremes, 2018, 3, 165-187.	3.9	21
41	Molecular dynamics studies of ion beam implantation and patterning of silicon: Effect of noble gas cluster formation. Physical Review B, 2018, 97, .	3.2	8
42	Latest Results From the Hybrid Illinois Device for Research and Applications (HIDRA). IEEE Transactions on Plasma Science, 2018, 46, 2685-2690.	1.3	13
43	Magnetic targeting of smooth muscle cells in vitro using a magnetic bacterial cellulose to improve cell retention in tissue-engineering vascular grafts. Acta Biomaterialia, 2018, 77, 172-181.	8.3	56
44	Titanium nitride formation by a dual-stage femtosecond laser process. Applied Physics A: Materials Science and Processing, 2018, 124, 1.	2.3	11
45	Studies of lithiumization and boronization of ATJ graphite PFCs in NSTX-U. Nuclear Materials and Energy, 2017, 12, 334-340.	1.3	12
46	Bacterial Nanocellulose Magnetically Functionalized for Neuroâ€Endovascular Treatment. Macromolecular Bioscience, 2017, 17, 1600382.	4.1	31
47	Grain size threshold for enhanced irradiation resistance in nanocrystalline and ultrafine tungsten. Materials Research Letters, 2017, 5, 343-349.	8.7	81
48	Massive-scale molecular dynamics of ion-irradiated III–V compound semiconductors at the onset of nanopatterning. Nuclear Instruments & Methods in Physics Research B, 2017, 409, 282-287.	1.4	2
49	Compatibility of lithium plasma-facing surfaces with high edge temperatures in the Lithium Tokamak Experiment. Physics of Plasmas, 2017, 24, .	1.9	28
50	Overview of NSTX Upgrade initial results and modelling highlights. Nuclear Fusion, 2017, 57, 102006.	3.5	45
51	Advances in boronization on NSTX-Upgrade. Nuclear Materials and Energy, 2017, 12, 744-748.	1.3	13
52	Unraveling the plasma-material interface with real time diagnosis of dynamic boron conditioning in extreme tokamak plasmas. Nuclear Fusion, 2017, 57, 086050.	3.5	11
53	Initial studies of plasma facing component surface conditioning in the national spherical tokamak experiment upgrade with the materials analysis particle probe. Nuclear Materials and Energy, 2017, 12, 1248-1252.	1.3	11
54	Deciphering surface behavior and deuterium retention in tin-lithium-coated fuzzy tungsten substrates. Nuclear Materials and Energy, 2017, 12, 1352-1357.	1.3	1

JEAN PAUL ALLAIN

#	Article	IF	CITATIONS
55	Unraveling atomic-level self-organization at the plasma-material interface. Journal Physics D: Applied Physics, 2017, 50, 283002.	2.8	16
56	Hydrogen retention in lithium on metallic walls from "in vacuo―analysis in LTX and implications for high-Z plasma-facing components in NSTX-U. Fusion Engineering and Design, 2017, 117, 135-139.	1.9	20
57	Nanostructured Biointerfaces. , 2017, , 41-72.		3
58	Unraveling wall conditioning effects on plasma facing components in NSTX-U with the Materials Analysis Particle Probe (MAPP). Review of Scientific Instruments, 2016, 87, 11D403.	1.3	9
59	Guest Editorial Special Issue on Symposium on Fusion Engineering. IEEE Transactions on Plasma Science, 2016, 44, 1463-1465.	1.3	Ο
60	Synthesis and <i>in vitro</i> safety assessment of magnetic bacterial cellulose with porcine aortic smooth muscle cells. Journal of Biomedical Materials Research - Part A, 2016, 104, 2801-2809.	4.0	7
61	Fabrication of a Functionalized Magnetic Bacterial Nanocellulose with Iron Oxide Nanoparticles. Journal of Visualized Experiments, 2016, , .	0.3	24
62	Dependence of LTX plasma performance on surface conditions as determined by in situ analysis of plasma facing components. Journal of Nuclear Materials, 2015, 463, 907-910.	2.7	26
63	Ion beam nanopatterning of III-V semiconductors: consistency of experimental and simulation trends within a chemistry-driven theory. Scientific Reports, 2015, 5, 18207.	3.3	42
64	HIDRA: Hybrid Illinois Device for Research and Applications. Fusion Science and Technology, 2015, 68, 497-500.	1.1	6
65	High flux irradiations of Li coatings on polycrystalline W and ATJ graphite with D, He, and He-seeded D plasmas at Magnum PSI. Journal of Nuclear Materials, 2015, 463, 1147-1151.	2.7	5
66	An <i>in vitro</i> model for preclinical testing of thrombogenicity of resorbable metallic stents. Journal of Biomedical Materials Research - Part A, 2015, 103, 2118-2125.	4.0	11
67	Sputtering of molybdenum and tungsten nano rods and nodules irradiated with 150eV argon ions. Applied Surface Science, 2015, 331, 299-308.	6.1	8
68	Kinetic Monte Carlo simulation of self-organized pattern formation induced by ion beam sputtering using crater functions. Physical Review B, 2015, 91, .	3.2	16
69	Early stage damage of ultrafine-grained tungsten materials exposed to low energy helium ion irradiation. Fusion Engineering and Design, 2015, 93, 9-14.	1.9	36
70	Addressing the Challenges of Plasma-Surface Interactions in NSTX-U. IEEE Transactions on Plasma Science, 2015, 43, 965-971.	1.3	1
71	An overview of recent physics results from NSTX. Nuclear Fusion, 2015, 55, 104002.	3.5	21
72	On the influence of space holder in the development of porous titanium implants: Mechanical, computational and biological evaluation. Materials Characterization, 2015, 108, 68-78.	4.4	56

#	Article	IF	CITATIONS
73	Development progress of the Materials Analysis and Particle Probe. Review of Scientific Instruments, 2014, 85, 11D835.	1.3	9
74	Differentiating the role of lithium and oxygen in retaining deuterium on lithiated graphite plasma-facing components. Physics of Plasmas, 2014, 21, .	1.9	14
75	Ultrafine tungsten as a plasma-facing component in fusion devices: effect of high flux, high fluence low energy helium irradiation. Nuclear Fusion, 2014, 54, 083013.	3.5	101
76	Helium Implantation of Ultrafine Grained Tungsten within a TEM. Materials Research Society Symposia Proceedings, 2014, 1645, 1.	0.1	0
77	In-situ TEM observation of the response of ultrafine- and nanocrystalline-grained tungsten to extreme irradiation environments. Scientific Reports, 2014, 4, 4716.	3.3	161
78	Atomistic simulation of ion beam patterning with crater functions. Nuclear Instruments & Methods in Physics Research B, 2013, 307, 189-193.	1.4	11
79	The role of oxygen in the uptake of deuterium in lithiated graphite. Journal of Applied Physics, 2013, 114,	2.5	10
80	Near sputter-threshold GaSb nanopatterning. Journal of Applied Physics, 2013, 114, 104308.	2.5	11
81	New biomaterial for treatment of penetrating brain injury (PBI) aneurysms: Nanostructured NiTi by directed irradiation synthesis (DIS). , 2013, , .		1
82	Overview of physics results from the conclusive operation of the National Spherical Torus Experiment. Nuclear Fusion, 2013, 53, 104007.	3.5	53
83	Surface chemistry analysis of lithium conditioned NSTX graphite tiles correlated to plasma performance. Fusion Engineering and Design, 2013, 88, 3157-3164.	1.9	17
84	Surface damage in ultrafine and multimodal grained tungsten materials induced by low energy helium irradiation. Journal of Nuclear Materials, 2013, 434, 170-177.	2.7	43
85	Characterization of fueling NSTX H-mode plasmas diverted to a liquid lithium divertor. Journal of Nuclear Materials, 2013, 438, S488-S492.	2.7	8
86	Nanopatterning of metal-coated silicon surfaces via ion beam irradiation: Real time x-ray studies reveal the effect of silicide bonding. Journal of Applied Physics, 2013, 113, .	2.5	20
87	Liquid lithium divertor characteristics and plasma–material interactions in NSTX high-performance plasmas. Nuclear Fusion, 2013, 53, 083032.	3.5	79
88	Recent progress in the NSTX/NSTX-U lithium programme and prospects for reactor-relevant liquid-lithium based divertor development. Nuclear Fusion, 2013, 53, 113030.	3.5	32
89	A new nanostructured material for regenerative vascular treatments: Magnetic bacterial nanocellulose (MBNC). , 2013, , .		3
90	Deuterium Uptake in Magnetic-Fusion Devices with Lithium-Conditioned Carbon Walls. Physical Review Letters, 2013, 110, 105001.	7.8	45

#	Article	IF	CITATIONS
91	Titanium surface modification by Directed Irradiation Synthesis (DIS): Nanostructuring for regenerative medicine. , 2013, , .		0
92	Overview of Innovative PMI Research on NSTX-U and Associated PMI Facilities at PPPL. Fusion Science and Technology, 2013, 63, 21-28.	1.1	1
93	Lithium-based surfaces controlling fusion plasma behavior at the plasma-material interface. Physics of Plasmas, 2012, 19, .	1.9	29
94	Real time x-ray studies during nanostructure formation on silicon via low energy ion beam irradiation using ultrathin iron films. Applied Physics Letters, 2012, 101, .	3.3	10
95	Materials analysis and particle probe: A compact diagnostic system for <i>in situ</i> analysis of plasma-facing components (invited). Review of Scientific Instruments, 2012, 83, 10D703.	1.3	33
96	The Materials Analysis Particle Probe (MAPP) Diagnostic System in NSTX. IEEE Transactions on Plasma Science, 2012, 40, 735-739.	1.3	9
97	In-situ ion scattering surface characterization of nanostructured materials exposed to controlled irradiation fields. Microscopy and Microanalysis, 2012, 18, 886-887.	0.4	1
98	Special Issue on Symposium on Fusion Engineering. IEEE Transactions on Plasma Science, 2012, 40, 550-551.	1.3	0
99	Dynamics of deuterium retention and sputtering of Li–C–O surfaces. Fusion Engineering and Design, 2012, 87, 1732-1736.	1.9	20
100	NSTX plasma operation with a Liquid Lithium Divertor. Fusion Engineering and Design, 2012, 87, 1724-1731.	1.9	72
101	Modeling of plasma/lithium-surface interactions in NSTX: Status and key issues. Fusion Engineering and Design, 2012, 87, 1737-1740.	1.9	7
102	Recent progress of NSTX lithium program and opportunities for magnetic fusion research. Fusion Engineering and Design, 2012, 87, 1770-1776.	1.9	11
103	The effect of native oxide on ion-sputtering-induced nanostructure formation on GaSb surfaces. Applied Physics Letters, 2012, 101, .	3.3	11
104	The effect of progressively increasing lithium coatings on plasma discharge characteristics, transport, edge profiles and ELM stability in the National Spherical Torus Experiment. Nuclear Fusion, 2012, 52, 083001.	3.5	101
105	In-situ probing of near and below sputter-threshold ion-induced nanopatterning on GaSb(100). Nuclear Instruments & Methods in Physics Research B, 2012, 272, 210-213.	1.4	24
106	Overview of physics results from NSTX. Nuclear Fusion, 2011, 51, 094011.	3.5	10
107	Lithium wall conditioning and surface dust detection on NSTX, and dust removal. Physica Scripta, 2011, T145, 014020.	2.5	1
108	Particle-induced damage effects on extreme UV (13.5-nm) source collector mirror optics. Proceedings of SPIE, 2011, , .	0.8	1

#	Article	IF	CITATIONS
109	Analysis of C-MOD molybdenum divertor erosion and code/data comparison. Journal of Nuclear Materials, 2011, 415, S112-S116.	2.7	20
110	Deuterium retention in NSTX with lithium conditioning. Journal of Nuclear Materials, 2011, 415, S773-S776.	2.7	19
111	Surface chemistry and physics of deuterium retention in lithiated graphite. Journal of Nuclear Materials, 2011, 415, S777-S780.	2.7	23
112	Chemical and physical erosion of carbon and metallic substrates containing lithium during low-energy deuterium ion irradiation. Journal of Nuclear Materials, 2011, 415, S133-S136.	2.7	11
113	NSTX plasma response to lithium coated divertor. Journal of Nuclear Materials, 2011, 415, S400-S404.	2.7	32
114	Multimodal grain size distribution and high hardness in fine grained tungsten fabricated by spark plasma sintering. Materials Science & Engineering A: Structural Materials: Properties, Microstructure and Processing, 2011, 528, 5670-5677.	5.6	82
115	Deuterium ion–surface interactions of liquid-lithium thin films on micro-porous molybdenum substrates. Nuclear Instruments & Methods in Physics Research B, 2011, 269, 1262-1265.	1.4	11
116	Formation of silicon nanodots via ion beam sputtering of ultrathin gold thin film coatings on Si. Nanoscale Research Letters, 2011, 6, 403.	5.7	19
117	The significance of <i>in situ</i> conditions in the characterization of GaSb nanopatterned surfaces via ion beam sputtering. Journal of Applied Physics, 2011, 110, .	2.5	21
118	The Materials Analysis patticle Probe (MAPP) diagnostic system in NSTX. , 2011, , .		0
119	Study of scalable IBS nanopatterning mechanisms for III-V semiconductors using in-situ surface characterization. Materials Research Society Symposia Proceedings, 2011, 1354, 127.	0.1	1
120	Lithium surface-response modelling for the NSTX liquid lithium divertor. Nuclear Fusion, 2011, 51, 023002.	3.5	21
121	Chemical response of lithiated graphite with deuterium irradiation. Journal of Applied Physics, 2011, 109, 053306.	2.5	35
122	Energetic Sn+ irradiation effects on ruthenium mirror specular reflectivity at 13.5-nm. Applied Physics A: Materials Science and Processing, 2010, 100, 231-237.	2.3	3
123	Lithium coatings on NSTX plasma facing components and its effects on boundary control, core plasma performance, and operation. Fusion Engineering and Design, 2010, 85, 865-873.	1.9	35
124	Special Issue on Symposium on Fusion Engineering. IEEE Transactions on Plasma Science, 2010, 38, 222-223.	1.3	0
125	Modeling of Surface Composition Dynamics in the ITER Divertor Region. IEEE Transactions on Plasma Science, 2010, 38, 414-418.	1.3	1
126	Modeling of beryllium-carbon dynamics in the ITER divertor region. , 2009, , .		0

8

#	Article	IF	CITATIONS
127	Progress in research and development of mirrors for ITER diagnostics. Nuclear Fusion, 2009, 49, 075014.	3.5	71
128	Experimental studies of lithium-based surface chemistry for fusion plasma-facing materials applications. Journal of Nuclear Materials, 2009, 390-391, 942-946.	2.7	35
129	Evaporated lithium surface coatings in NSTX. Journal of Nuclear Materials, 2009, 390-391, 1000-1004.	2.7	74
130	â€~Mixed-material evolution analysis of the ITER divertor'. Journal of Nuclear Materials, 2009, 390-391, 123-126.	2.7	6
131	Reactivity of lithium exposed graphite surface. Applied Surface Science, 2009, 255, 8539-8543.	6.1	36
132	Overview of results from the National Spherical Torus Experiment (NSTX). Nuclear Fusion, 2009, 49, 104016.	3.5	41
133	Plasma–surface interaction issues of an all-metal ITER. Nuclear Fusion, 2009, 49, 035007.	3.5	78
134	Specular reflectivity of 13.5-nm light from Sn islands deposited on grazing incidence mirror surfaces. Applied Physics A: Materials Science and Processing, 2008, 91, 13-16.	2.3	4
135	The effect of lithium surface coatings on plasma performance in the National Spherical Torus Experiment. Physics of Plasmas, 2008, 15, .	1.9	153
136	Particle deposition and optical response of ITER motional Stark effect diagnostic first mirrors. Nuclear Fusion, 2008, 48, 045003.	3.5	23
137	Collisional and thermal effects on liquid lithium sputtering. Physical Review B, 2007, 76, .	3.2	42
138	IMPACT: A facility to study the interaction of low-energy intense particle beams with dynamic heterogeneous surfaces. Review of Scientific Instruments, 2007, 78, 113105.	1.3	26
139	Effects of a liquid lithium curtain as the first wall in a fusion reactor plasma. Chinese Physics B, 2007, 16, 3312-3318.	1.3	4
140	Energetic and thermal Sn interactions and their effect on EUVL source collector mirror lifetime at high temperatures. , 2007, , .		5
141	Debris and radiation-induced damage effects on EUV nanolithography source collector mirror optics performance. , 2007, , .		6
142	Near-surface bipartition model for the study of material response of plasma-facing surfaces exposed to energetic charged particles. Nuclear Instruments & Methods in Physics Research B, 2007, 259, 847-852.	1.4	5
143	Divertor and midplane materials evaluation system in DIII-D. Journal of Nuclear Materials, 2007, 363-365, 276-281.	2.7	10
144	Effect of charged-particle bombardment on collector mirror reflectivity in EUV lithography devices. , 2006, 6151, 837.		9

#	Article	IF	CITATIONS
145	Surface erosion by highly-charged ions. Nuclear Instruments & Methods in Physics Research B, 2006, 242, 498-502.	1.4	11
146	Xe+-irradiation effects on multilayer thin-film optical surfaces in EUV lithography. Nuclear Instruments & Methods in Physics Research B, 2006, 242, 520-522.	1.4	10
147	Plasma-material Interaction Studies On Lithium And Lithiated Substrates During Compact Tokamak Operation. AIP Conference Proceedings, 2006, , .	0.4	1
148	Erosion/redeposition analysis of the ITER first wall with convective and non-convective plasma transport. Physics of Plasmas, 2006, 13, 122502.	1.9	18
149	Overview of the ALPS Program. Fusion Science and Technology, 2005, 47, 669-677.	1.1	28
150	Plasma/Liquid-Metal Interactions During Tokamak Operation. Fusion Science and Technology, 2005, 47, 686-697.	1.1	11
151	PSI modeling of liquid lithium divertors for the NSTX tokamak. Journal of Nuclear Materials, 2005, 337-339, 1053-1057.	2.7	22
152	Model development and analysis of temperature-dependent lithium sputtering and sputtered Li+ transport for tokamak plasma-facing applications. Journal of Nuclear Materials, 2005, 337-339, 94-98.	2.7	11
153	A model for ion-bombardment induced erosion enhancement with target temperature in liquid lithium. Nuclear Instruments & Methods in Physics Research B, 2005, 239, 347-355.	1.4	9
154	Erosion, transport, and tritium codeposition analysis of a beryllium wall tokamak. Fusion Engineering and Design, 2005, 72, 363-375.	1.9	8
155	Ion-Induced Surface Modification of EUV and VUV Plasma-Facing Collector Mirrors. Materials Research Society Symposia Proceedings, 2005, 908, 1.	0.1	2
156	Interaction of Impurity (Li, Be, B and C) and Hydrogen Isotope Pellet Injection with Reactor-relevant Plasmas. Plasma Science and Technology, 2005, 7, 2615-2622.	1.5	1
157	Lithium erosion experiments and modelling under quiescent plasma conditions in DIII-D. Nuclear Fusion, 2004, 44, 655-664.	3.5	49
158	Radiation-induced synergistic effects of athermal and thermal mechanisms on erosion and surface evolution of advanced electrode and condenser optics materials. , 2004, , .		10
159	Studies of liquid-metal erosion and free surface flowing liquid lithium retention of helium at the University of Illinois. Fusion Engineering and Design, 2004, 72, 93-110.	1.9	18
160	Experimental observations of lithium as a plasma-facing surface in the DIII-D tokamak divertor. Fusion Engineering and Design, 2004, 72, 133-147.	1.9	49
161	Temperature dependence of liquid Sn sputtering by low-energy He+ and D+ bombardment. Journal of Nuclear Materials, 2004, 335, 115-120.	2.7	22
162	Experimental investigation of materials damage induced by hot Xe plasma in EUV lithography devices. ,		4

2004, , .

#	Article	IF	CITATIONS
163	D+, He+ and H+ sputtering of solid and liquid phase tin. Journal of Nuclear Materials, 2003, 313-316, 636-640.	2.7	22
164	Temperature dependence of liquid-lithium sputtering from oblique 700 eV He ions. Journal of Nuclear Materials, 2003, 313-316, 641-645.	2.7	31
165	Helium retention and diffusivity in flowing liquid lithium. Journal of Nuclear Materials, 2003, 313-316, 646-650.	2.7	13
166	Experimental Measurements of Helium Retention in Flowing Liquid Lithium. Fusion Science and Technology, 2003, 44, 232-236.	1.1	2
167	Measurements and modelling of solid phase lithium sputtering. Nuclear Fusion, 2002, 42, 202-210.	3.5	64
168	FLIRE—flowing liquid surface retention experiment, design and testing. Fusion Engineering and Design, 2002, 61-62, 245-250.	1.9	13
169	Enhancement of aluminum oxide physical vapor deposition with a secondary plasma. Surface and Coatings Technology, 2002, 149, 161-170.	4.8	22
170	Deuterium Treatment Effects On Lithium And Tin-Lithium Sputtering In Solid And Liquid Phase. , 2002, , 73-82.		3
171	Collisional Transport in Magnetized Plasmas, by Per Helander and Dieter J. Sigmar. Cambridge University Press, 2002. 292 pages. ISBN 0521807980. £70 Journal of Plasma Physics, 2002, 68, 237-240.	2.1	1
172	Emerging viruses and transfusion. Transfusion Clinique Et Biologique, 2001, 8, 220-221.	0.4	3
173	Absolute sputtering yield of Ti/TiN by Ar+/N+ at 400–700 eV. Journal of Vacuum Science and Technology A: Vacuum, Surfaces and Films, 2001, 19, 1004-1007.	2.1	38
174	D, He and Li sputtering of liquid eutectic Sn–Li. Journal of Nuclear Materials, 2001, 290-293, 33-37.	2.7	42
175	Measurements and modeling of D, He and Li sputtering of liquid lithium. Journal of Nuclear Materials, 2001, 290-293, 180-184.	2.7	39
176	Erosion/redeposition analysis of lithium-based liquid surface divertors. Journal of Nuclear Materials, 2001, 290-293, 185-190.	2.7	38
177	ALPS–advanced limiter-divertor plasma-facing systems. Fusion Engineering and Design, 2000, 49-50, 127-134.	1.9	67
178	Fundamentals of Plasma-Material Interactions in Magnetic Fusion Devices. , 0, , .		2
179	Design and Analysis of an Advanced Three-Point Bend Test Approach for Miniature Irradiated Disk Specimens. Fusion Science and Technology, 0, , 1-8.	1.1	1
180	Irradiation Effects on EUV Nanolithography Collector Mirrors. , 0, , .		2